The Reduction of Al_2O_3 to Aluminum in a Plasma

ROGER K. RAINS AND ROBERT H. KADLEC

The reduction of aluminum oxide to aluminum in radio frequency generated plasmas was studied experimentally. Argon with hydrogen, carbon dioxide, and methane were used as plasma gases. Product was collected from the reactor walls and/or cold-finger collectors. Gaseous quenching was also investigated, using hydrogen, methane, and carbon dioxide. Conversions up to 50 pct were determined using wet chemistry. Optical and X-ray methods confirmed the species present during and after reaction. The effects of particle size, flow rates, and power input were determined. Solutions of energy, momentum, and mass balances yield a qualitative explanation of the process. Vaporization rate controls.

THE primary aim of this research was to investigate the reduction of Al_2O_3 to aluminum in radio frequency generated, induction coupled plasmas. It was also intended to demonstrate that an induction-coupled plasma reactor is especially suitable for such gas-solid reactions. The conversion of Al_2O_3 to aluminum in this study was effected in argon, Ar-H_2, Ar-CO, and Ar-CH_4 plasmas. Different quench techniques and three reaction variables were investigated.

Several investigators[1-5] have attempted plasma reductions of metallic oxides, chlorides, and sulfides. Their work demonstrates that the reduction of metallic oxides in plasmas is feasible. The extent of the reduction depends on the oxide particle size, the oxide flow rate, and the power input to the plasma. It is apparent that the lack of success with Al_2O_3 was due to the use of particle sizes and flow rates that were too great.

The gaseous aluminum suboxides are of interest since they are expected to occur either during the dissociation of Al_2O_3 or by a recombination of aluminum and oxygen atoms. It is concluded from an examination of the literature[6] that AlO and Al_2O are the only two important gaseous oxides of aluminum. The former is the principal gaseous suboxide under neutral or oxidizing conditions and the latter predominates under reducing conditions. There has been no conclusive evidence that solid suboxides can exist at room temperature[6] but solid AlO and Al_2O have been identified between 1100° and 1600°C.[7] However, this does not preclude the possibility of the formation of a solid suboxide from the rapid quench of the gaseous oxide.

THEORETICAL CONSIDERATIONS

In the nonreducing environment of an argon plasma, Al_2O_3 will vaporize to AlO and oxygen. The optimum temperature for the dissociation

$$Al_2O_3 \rightarrow 2AlO + O \qquad [1]$$

is about 4000°K.[8-11] But Fig. 1[12] shows that AlO is unstable above 4400°K and since temperatures in excess of 10,000°K are present in an argon plasma, the AlO will further dissociate:

$$AlO \rightarrow Al + O \qquad [2]$$

shortly after its formation.

When a reducing gas (such as H_2, CO, or CH_4) is added to the argon plasma, the Al_2O_3 dissociation is to Al_2O and oxygen:

$$Al_2O_3 \rightarrow Al_2O + 2O \qquad [3]$$

Again, from Fig. 1, it is seen that Al_2O is unstable above 4300°K, so it also decomposes:

$$Al_2O \rightarrow 2Al + O \qquad [4]$$

In either case, therefore, the plasma core will contain aluminum and oxygen atoms instead of AlO or Al_2O molecules.

Once free aluminum is obtained, it must be removed from the plasma before it can be reoxidized in the cooler tail flame. This is done by condensing

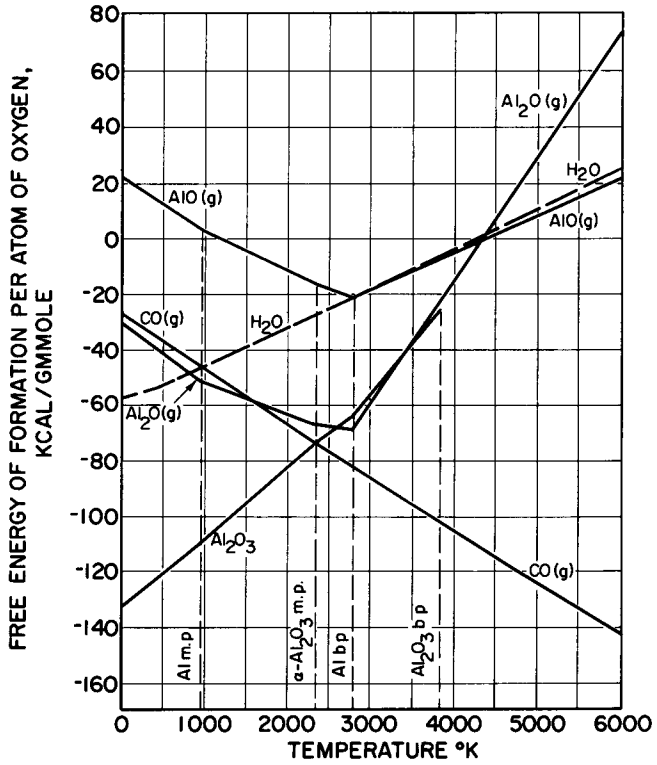

Fig. 1—Free energy of formation per atom of oxygen vs temperature for various compounds.

ROGER K. RAINS, formerly at the University of Michigan, Ann Arbor, Mich., is with the Monsanto Company, St. Louis, Mo.
ROBERT H. KADLEC is Associate Professor of Chemical Engineering, University of Michigan.

Manuscript submitted January 5, 1970

the aluminum onto a water-cooled surface: either the reactor wall or a probe inserted into the plasma core. The concentration and temperature gradients are very steep in this "quench region" between the plasma core and the cool surface. A condensable species entering the quench region is condensed with extreme rapidity. If this rate of condensation is greater than the rate of oxidation in the quench region, free aluminum is obtained.

The recovery of aluminum can be improved by increasing the rate of transport of aluminum through the plasma to the quench region. The radial molar flux of aluminum in a mixture of aluminum and the noncondensable species in an argon plasma is:

$$N_{\mathrm{Al}\,r} = \frac{C D_{\mathrm{Al}\,m}}{1 - X_{\mathrm{Al}}} \frac{\partial X_{\mathrm{Al}}}{\partial r} \qquad [5]$$

The other gases present in the quench region are assumed to form a stagnant film in the derivation of Eq. [5]. It is seen that the molar flux of aluminum increases with both the concentration and temperature of aluminum ($D_{\mathrm{Al}\,m}$ increases with temperature). So, the recovery of aluminum from an Al-O-Ar plasma can be increased by increasing either the concentration or the temperature of the aluminum in the plasma.

The addition of H_2, CH_4, or CO to the plasma is expected to aid the recovery of aluminum. In the hot plasma core, these gases dissociate to their elements. Thus, atomic hydrogen or carbon is present in the plasma. The carbon will condense along with aluminum in the quench region. Oxygen prefers carbon to aluminum, as seen by a comparison of the free energies of formation of CO, AlO, and Al_2O in Fig. 1. Therefore, carbon should effectively remove oxygen during the quench; thus diminishing the chance that the aluminum will oxidize. Hydrogen, on the other hand, has less affinity for oxygen than does aluminum over fairly large ranges in temperature. Therefore, hydrogen should be of little benefit in removing oxygen during the quench.

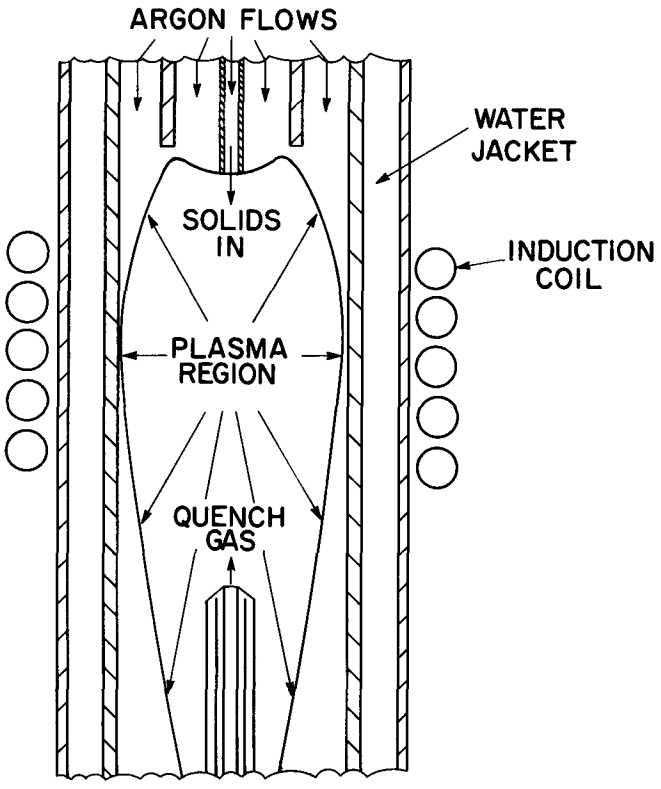

Fig. 2—Plasma reactor.

The history of a small Al_2O_3 particle in an argon plasma was estimated from a computer solution of unsteady state heat, mass, and momentum balance equations for the particle. The momentum balance derived for a small particle injected into the plasma is:

$$\frac{d^2 z}{dt^2} = \pm \tfrac{3}{4} C_D \frac{\rho_\infty}{d_s \rho_s} \left(\frac{dz}{dt} - v_\infty\right)^2 + g \qquad [6]$$

The energy balance for a particle as it is being heated to its vaporization temperature is:

$$\tfrac{1}{6} \rho_s d_s C_{ps} \frac{dT_s}{dt} = h(T - T_s) - \sigma e_s T_s^4 \qquad [7]$$

Vaporization of the solid particle to AlO and oxygen is described by the combined heat and mass balance equation:

$$-\tfrac{1}{2} \Delta H_r^\circ \rho_s \frac{d(d_s)}{dt} = h(T - T_s) - \sigma e_s T_s^4 \qquad [8]$$

where ΔH_r° = heat of reaction for dissociation to aluminum and oxygen (since the AlO initially formed quickly dissociates to aluminum and oxygen).

The heat transfer coefficient used in Eqs. [7] and [8] is:[13]

$$h = \frac{k_f}{d_s} (2 + 0.6 \mathrm{Re}_f^{0.5} \mathrm{Pr}_f^{0.3}) \qquad [9]$$

The relative velocity of the particle is used in evaluating the Reynolds number. The two terms on the right hand side of Eq. [9] represent the conductive and convective contributions, respectively. Thermal radiation effects from the plasma can be neglected.[14] The average boundary layer temperature at which the gas properties are evaluated is that which corresponds to the reference enthalpy given by:

$$h_{\mathrm{ref}} = 0.5(h_\infty - h_s) + h_s \qquad [10]$$

This reference enthalpy method is suggested by Eckert[15] for the case of a large temperature difference across the boundary layer.

EXPERIMENTAL APPARATUS AND PROCEDURES

The radio frequency, induction-coupled plasmas were generated and contained in the water-cooled quartz reactor diagramed in Fig. 2. The majority of the argon was fed tangentially (the outer two arrows on Fig. 2) to provide vortex stability. Additional argon was fed axially to provide a sheath for the oxide powder as it entered the plasma. This helped to keep the powder on the centerline of the plasma. The remaining argon was used as carrier gas for the solids and was introduced axially through an alumina powder feed tube. Whenever H_2, CO, or CH_4 was used in the plasma, it was introduced with the tangential argon.

The radio frequency power for the plasma was provided by a 23.5 kva; 3 Mc Lepel generator. By passing the radio frequency current through a five turn induction coil, a 3 Mc alternating electromagnetic field was produced and electrodeless discharge could be obtained.

A maximum power input to the plasma of about 10 kw was attainable. The plasma column was initiated with the high voltage discharge of a tesla coil. A 3.4 m focal length Ebert Mark IV stigmatic plane grating spectrograph was used to analyze the radiation from the plasma.

Quench probes were used both to augment the recovery of product by collection on its outer wall and to introduce quench gases countercurrent to the plasma flow. To meet this dual need, water-cooled probes consisting of three concentric stainless tubes were used.

The three variables that were studied in detail were the Al_2O_3 particle size, Al_2O_3 mass flow rate, and power input to the plasma. The first two were varied at a constant power input level. The effect of the last was determined by varying the power input level for a constant Al_2O_3 flow rate and particle size.

The effects of H_2, CO, and CH_4 were studied in two ways. First, the gas was fed directly into the plasma along with the argon. A single run was made with each of the gases. Second, the gas was fed through the quench probe countercurrent to the plasma. For this case, several H_2 flow rates and one each for CO and CH_4 were used.

For the above experiments, the conversion of Al_2O_3 to aluminum was based on the amount of product collected on the reactor wall instead of the Al_2O_3 input flow rate. No attempt was made to collect all the material that was fed to the reactor. Water-cooled quench probes were then used to show that it would be possible to increase the recovery without lowering the conversion. The probes were positioned directly in the plasma so that the tip was about $\frac{3}{4}$ in. below the coil, see Fig. 2.

The amount of aluminum in the product was determined by a wet chemical procedure. After dissolving the aluminum in HCl, it was precipitated as aluminum quinolate by using an excess of 8-quinolinol. The precipitate was redissolved in half concentrated HCl, reforming 8-quinolinol. This was brominated with a $KBrO_3$-KBr solution, liberating Br_2, and then an excess of KI was added. The resulting iodine was titrated with thiosulfate to the starch end point. This method is discussed in greater detail by Kolthoff and Belcher.[16]

Argon and aluminum temperatures were determined spectrographically. Certain species of these are electronically excited in the plasma, thus emitting radiation. The intensity of this radiation depends on both the temperature of the emittor and the wavelength of the radiation. Only certain wavelengths occur for a given element, and these are characteristic of the element. By measuring the absolute intensity at a given wavelength with an optical spectrograph, the temperature is obtained. It is thus possible to obtain a temperature for each species in the plasma.

EXPERIMENTAL RESULTS AND ANALYSIS

Aluminum-containing species were identified at various points in the argon plasma and tail flame by use of the spectrograph. The plasma core consisted only of atomic and ionic species. This hot core was surrounded by a thin region containing AlO and aluminum. Both AlO and aluminum were also detected throughout the cooler tail flame of the plasma.

A rigorous group III qualitative chemical analysis of product obtained from the reduction of Al_2O_3 in an argon plasma gave a positive test for aluminum. The presence of aluminum in the product was confirmed by an X-ray diffraction analysis. The only diffraction lines in addition to the aluminum lines were due to α-Al_2O_3, γ-Al_2O_3, and the impurities that were present in the reactant alumina. Thus, it is certain that aluminum is the reduction product of Al_2O_3 instead of a solid aluminum suboxide. This aluminum was found to be finely divided and highly pyrophoric.

Products from the reduction of Al_2O_3 in Ar-CO and Ar-CH_4 plasmas were also analyzed to determine the nature of the products. Both gave positive qualitative tests for aluminum and both contained a considerable amount of carbon. Diffraction analysis of the product from the Ar-CO reduction identified aluminum, α-Al_2O_3, and γ-Al_2O_3. The Ar-CH_4 reduction product also contained Al_4C_3. The aluminum oxycarbides, Al_2OC and Al_4O_4C, were not found in either case nor were solid aluminum suboxides.

The variation of percent conversion with alumina flow rate for the particle sizes used is shown in Fig. 3. A single run was also made with 60 mesh (250 μ) alumina flowing at 0.19 g per min. In this case, there was no aluminum in the product nor was there any spectroscopic evidence of gaseous aluminum in the plasma. The 500 mesh oxide gave a higher conversion than the 400 mesh alumina throughout the entire range of flow rates that were used. This is probably because the smaller 500 mesh particle vaporizes more completely than the 400 mesh oxide under the same conditions.

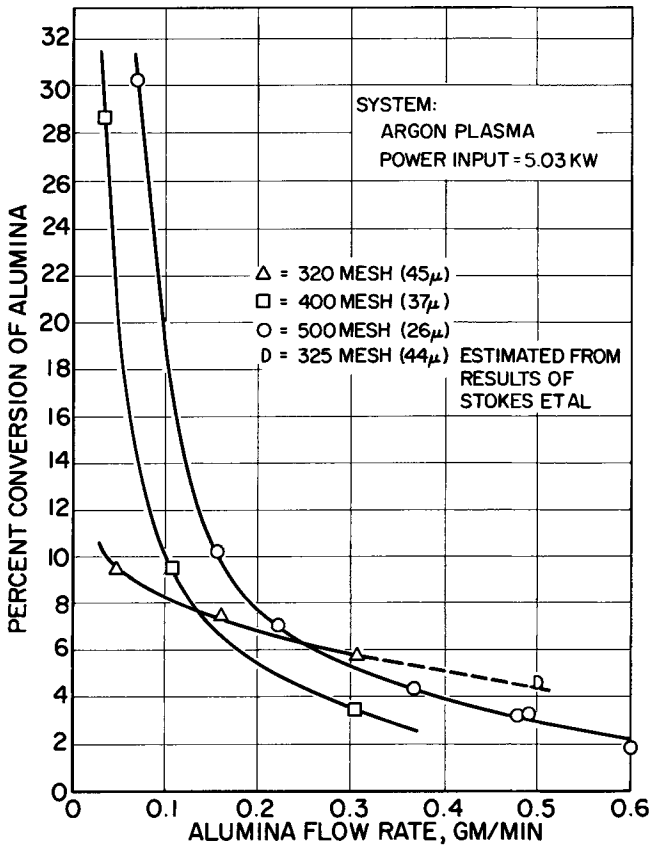

Fig. 3—Variation of the conversion of Al_2O_3 in an argon plasma with the Al_2O_3 flow rate and particle size.

The increase in conversion with a decrease of solids flow rate, obtained for all three particle sizes, is also reasonable. At lower alumina mass flow rates, fewer particles are present in any section of the plasma at a given time. This means that energy is transferred from the plasma to each particle more efficiently and more of the particle is vaporized.

Conversely, as the alumina mass flow rate increases, the efficiency of the energy transfer to a given particle decreases. So a smaller percentage of the alumina is vaporized and the conversion drops. The larger the particle, however, the less noticeable is this effect. This is because the number density of oxide particles in the plasma decreases as the particle diameter increases. Eventually, this can result in higher conversions for larger particles than for smaller particles at high flow rates. This is in fact exhibited by the behavior of the 320 mesh oxide.

At very low flow rates, single particle flow is approached. In this case, the efficiency of the energy transfer is no longer important. Instead, the true diameter effect is observed. That is, conversions obtained at very low flow rates agree qualitatively with the extents of vaporization predicted by the computer solutions of the heat, mass, and momentum balances.

The variation of conversion with power input is given in Fig. 4. As the power level increase, the Al_2O_3 particles are more completely vaporized and the concentration of aluminum in the plasma is greater. In addition, the aluminum temperature is higher so that the aluminum has a greater diffusivity. Both effects can increase the molar flux of aluminum to the quench region, and hence, increase the recovery.

The use of H_2 in the plasma caused only a slight increase in the percent conversion of Al_2O_3. But with CO, the conversion was twice that obtained with argon alone. And with CH_4, the conversion was quadrupled. These results confirm the earlier discussion concerning the effect of carbon vs hydrogen. Carbon is simply much more effective than hydrogen.

In the above experiments, there was no attempt to collect all the material fed to the plasma. In some runs, water-cooled probes were inserted into the plasma and additional product was recovered. The conversions based upon the material collected on these probes were actually greater than those for the product on the reactor wall. So the quench probes can be used not only to recover additional material but to increase the conversion as well. The probes are inserted directly into the plasma core, where the aluminum concentration is the highest. Therefore, more aluminum is available to condense on the probes than on the wall.

The probes were also used for feeding H_2, CO, and CH_4 into the lower section of the plasma core countercurrent to the plasma flow. Once again, hydrogen was of little benefit, as is seen in Fig. 5, but both CO and CH_4 doubled the conversions obtained with only argon. This further illustrates that carbon helps to prevent oxidation of aluminum during the quench.

Argon temperatures, determined at the power levels in Fig. 4, were 10,900°, 11,100°, and 11,200°K. The corresponding plasma enthalpy range is 1900 to 2100 cal per g.[17] So a modest 3 pct increase in temperature results in a 10 pct rise in the enthalpy. The measured aluminum temperatures were somewhat lower than anticipated. But in general, higher temper-

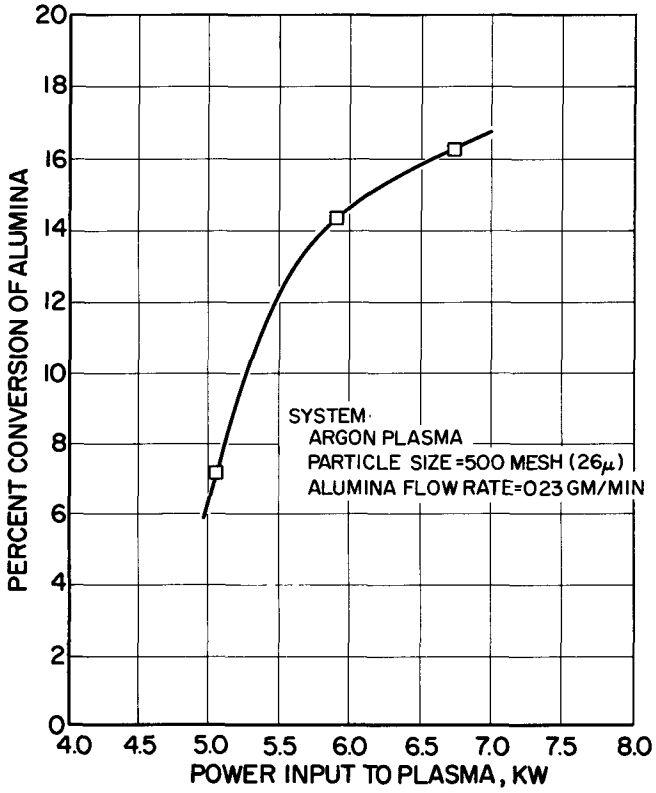

Fig. 4—Effect of power input upon the conversion of Al_2O_3 to aluminum in an argon plasma.

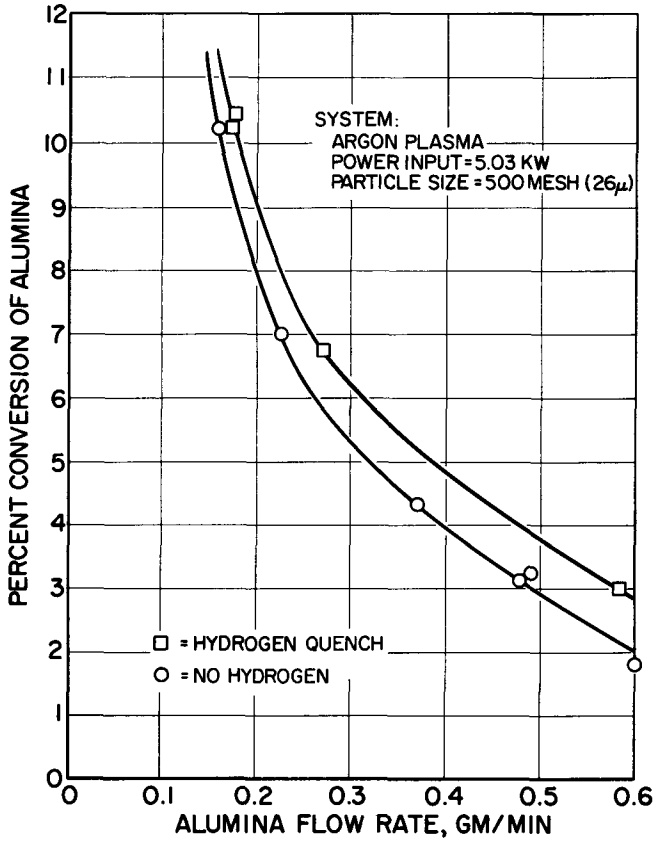

Fig. 5—Comparison of conversions obtained with and without the use of hydrogen as a quench gas.

atures were obtained at greater power input levels and lower alumina flow rates.

Computer solutions of heat, mass, and momentum balances for aluminum oxide particles in an argon plasma estimate the amount of alumina that will vaporize. This is reported as percent vaporized, which is 100 times the volume vaporized divided by the initial volume for a spherical particle. The conversions for 320, 400, and 500 mesh alumina at a flow rate of 0.06 g per min, taken from Fig. 3, are compared with the percents vaporized, determined for the same plasma conditions, in Fig. 6. Since the curves have the same shape, it appears that the conversion depends directly on the extent to which the alumina is vaporized. This explains the poor results obtained by earlier investigators:[1,2] they simply did not produce enough gaseous aluminum with the flow rates and particle sizes they used.

SUMMARY AND CONCLUSIONS

The reduction of aluminum oxide to aluminum in an atmospheric, induction-coupled argon plasma was studied experimentally. The conversion of the alumina was based upon the amount of Al_2O_3 and aluminum collected on the reactor wall. The variation of conversion with alumina particle size, alumina mass flow rate and the power input to the plasma was determined. Particle sizes of 500 mesh (26 μ), 400 mesh (37 μ), and 320 mesh (45 μ); flow rates of 0.03 to 0.6 g per min; and power inputs of 5.03, 5.86, and 6.69 kw were used. These power levels correspond to argon temperatures of 10,900°, 11,100°, and 11,200°K, respectively. With argon plasmas, the conversions (ranging from 3 to 30 pct) were generally found to increase with decreasing alumina flow rate and particle size and with increasing power input. The improvements in the conversion were due to increases in the amount of the oxide vaporized. The results agree qualitatively with the amount of alumina vaporization predicted by computer solutions to heat, mass, and momentum balances for the oxide. The conversions obtained can be explained on the basis of a diffusion controlled quench of aluminum atoms.

The use of water-cooled probes placed directly in the plasma allowed the recovery of additional aluminum at higher conversions. This indicates that with a reactor designed to collect a maximum amount of product, the conversions obtained in this work will be maintained or even improved. It was also possible to enhance the conversion by using CO and CH_4 in the plasma with the argon and as quench gases introduced into the lower section of the plasma core countercurrent to the plasma flow. Doubling and quadrupling of the conversion was obtained in this way. The use of H_2 in each application was of little benefit. The relative effect of carbon and H_2 as oxygen scavengers explains the results.

Wet chemical and X-ray diffraction analyses of the reduction product from argon and Ar-CO plasmas identified aluminum, α-Al_2O_3, and γ-Al_2O_3. Similar analyses of product from an Ar-CH_4 plasma indicated that aluminum and Al_4C_3 were present in addition to the oxides. No solid aluminum suboxides or aluminum oxycarbides were found.

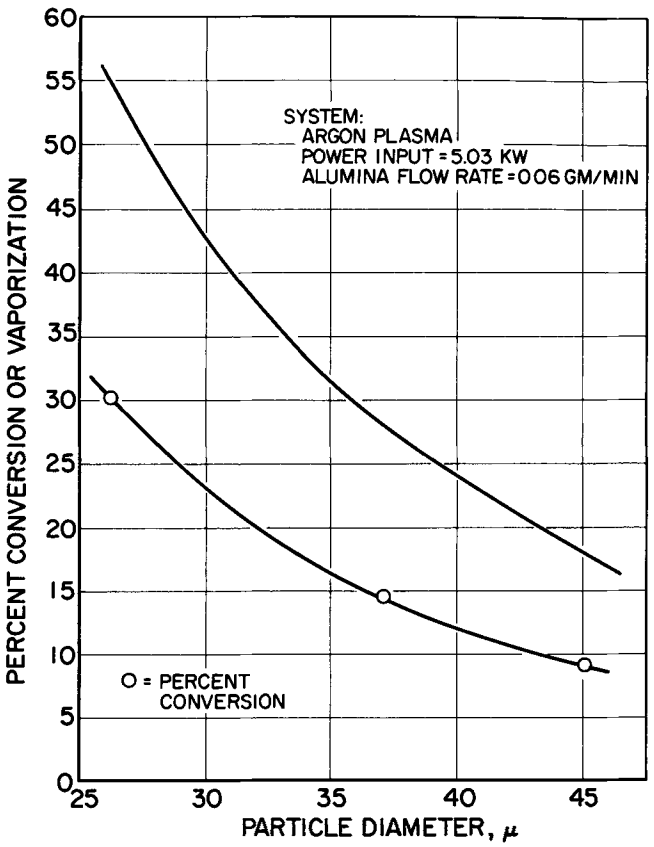

Fig. 6—Comparison of the percents of conversion and vaporization obtained with 26, 37, and 45 μ Al_2O_3 particles.

The reduction of aluminum oxide with appreciable conversion has been demonstrated to be quite feasible in an induction-coupled plasma reactor. It should be possible, on the basis of the results of this study, to achieve equal success in the reduction of other metallic oxides that are as stable as alumina.

ACKNOWLEDGMENT

The authors wish to express their appreciation to the Bethlehem Steel Co. for financial support of this work.

NOMENCLATURE

Symbols

A	area—sq cm
C	total concentration—gmol per cu cm
C_D	drag coefficient
C_P	heat capacity—cal per g-°K
d	diameter—cm
D_{im}	effective binary diffusivity for diffusion of i in a mixture—sq cm per sec
e	emissivity
g	gravitation acceleration—cm per sq sec
h	heat transfer coefficient—cal per sec-sq cm-°C
h	specific enthalpy—cal per g

h_{ref}	specific enthalpy at reference temperature in film around a solid particle—cal per g
ΔH_r°	heat of reaction—cal per g
k	thermal conductivity—cal per sec-cm-°C
N_{ir}	radial molar flux of i—gmol per sq cm-sec
Pr	Prandtl number
r	radial position—cm
Re	Reynolds number
t	time particle has been in plasma—sec
T	absolute temperature—°K
v	velocity—cm per sec
v_{rel}	velocity of solid particle relative to the plasma—cm per sec
X_i	mole fraction of i
z	axial position in plasma—cm
ρ	density—g per cu cm
σ	Stefan-Boltzmann constant—cal per sec-sq cm-°K^4

Subscripts

f	film or boundary layer around a solid particle in plasma
s	solid particle
∞	bulk plasma

REFERENCES

1. A. V. Grosse, H. W. Leutner, and C. S. Stokes: First Annual Report, Office of Naval Research, Task No. NR 052-429, 1961, pp. 27–29.
2. C. S. Stokes, J. A. Cahill, J. J. Correa, and A. V. Grosse: Final Report, Air Force Office of Scientific Research, AFOSR-62-196, 1964, pp. 19–31.
3. R. A S. Brown: Paper at the CIMM, Conference of Metallurgists, Kingston, Ontario, 1967, p. 13.
4. G. E. Biggerstaff, W. R. Golliher, R. L. Harris, and W. R. Rossmassler: AEC R and D Report, KY-453, 1964, pp. 4–20.
5. P. A. Huska and C. W. Clump: *I and EC Process Design and Development,* 1967, vol. 6, pp. 238–44.
6. R. K. Rains. Ph. D. thesis, The University of Michigan, 1968, pp. 4–6, Available from University Microfilms, Ann Arbor, Mich.
7. M. Hoch and H. L. Johnston: *J Am. Chem. Soc*, 1954, vol. 76, pp. 2560–1.
8. F. P. Coheur and P. Coheur: *Chem. Zentr.*, 1944, vol. 1, p. 978.
9. F. P. Coheur and P. Coheur *Rev. Universelle Mines,* 1943, vol. 19, pp. 86–89.
10. P. Coheur: *Bull Classe Sci., Acad. Roy. Belg.*, 1942, vol. 28, pp. 569–73.
11. L. Brewer and A. W. Searcy *J. Am. Chem. Soc*, 1951, vol 73, pp. 5308–14.
12. *JANAF Thermochemical Tables,* Dow Chemical Co., 1965.
13. R. B. Bird, W. E. Stewart, and E. N. Lightfoot: *Transport Phenomena,* p. 409, John Wiley & Sons, Inc., New York, 1960.
14. G R. Chludzinski: Ph. D. thesis, The University of Michigan, 1964, pp. 144–52, Available from University Microfilms, Ann Arbor, Mich.
15. E. R. G. Eckert: *J. Aero Sci*, 1955, vol. 22, pp. 585–87.
16. I. M. Kolthoff and R. Belcher *Volumetric Analysis,* vol. 3, pp. 552–54, Interscience Publishers, Inc., New York, 1957
17. K S. Drellishak, C. F. Knopp, and A. B. Cambel: Technical Documentary Report, AEDC-TDR-63-146, 1963, pp. 119–20.